

THE FEASIBILITY OF FUSING SATELLITE IMAGERIES FOR HIGH-FREQUENCY SEA LEVEL MONITORING

**Andriani Putri¹, Sri Azizah Nazhifah², Abdurrahman Ridho³,
Hayatun Maghfirah⁴, Cut Mutia⁵, Cukri Rahmi Niani⁶, Sanusi⁷**

^{1,3,4,5,6,7} Teknologi Informasi, Fakultas Teknik, Universitas Teuku Umar,
Meulaboh, Indonesia

² Informatika, Fakultas Matematika dan Ilmu Pengetahuan Alam,
Universitas Syiah Kuala, Banda Aceh, Indonesia

E-mail: ¹andrianiputri@utu.ac.id, ²sriazizah07@usk.ac.id,
³abdurrahman.ridho@utu.ac.id, ⁴hayatunmaghfirah@utu.ac.id, ⁵cutmutia@utu.ac.id,
⁶cukrirahminiani@utu.ac.id, ⁷sanusi@utu.ac.id

Abstract

Enhancing the capacity to monitor swift environmental shifts at finer scales requires satellite image that offers high spatial and temporal resolution. However, no individual satellite can offer images meeting both criteria simultaneously. To tackle this challenge, spatial temporal fusion algorithms have been developed to derive fine-scale and time-series images. Conversely, effective monitoring of water levels is crucial for preventing natural disaster, such as flood and tsunami mitigation. Yet, monitoring these natural changes regularly poses challenges for remote sensing satellites, given their limitations in either spatial or temporal resolution. For instance, the spatial resolution of 30 meters of Landsat 8 provides imagery with a but lacks the temporal resolution needed to capture dynamic events. On the contrary, the Himawari 8 has the capability to monitor the entire hemisphere every 10 minutes. However, its inadequate resolution affects the precision of sea water change mapping. This research seeks to utilize Landsat OLI and Himawari-8 images jointly for tracking sea level variation patterns. Our approach involves calculating a water index from both Landsat and Himawari images, then using an image fusion algorithm to merge these indices. Next, we identify water coverage by applying a specific threshold on the water index. The comparison of water percentages with reference water height observations has delivered encouraging outcomes.

Keywords: *image fusion, sea level monitoring, water index*

1. Introduction

Recent advancements in remote sensing have transformed the way high-resolution images are obtained, unlocking numerous potential applications. One notable application is the tracking of sea level changes, which is essential for managing natural disasters such as floods and tsunamis [1]. Sea level, referring to the average height of the ocean surface between high and low tides, has a direct impact on coastal ecosystems and freshwater reserves as it increases. Therefore, monitoring sea level is vital for efficient disaster preparedness. While traditional methods like water gauge stations are effective, they are limited by their low spatial resolution and scattered deployment. To address these challenges, remote sensing technologies have been utilized since the 1970s. Instruments such as MODIS and Landsat Enhanced Thematic Mapper Plus (ETM+) have played a

**THE FEASIBILITY OF FUSING SATELLITE IMAGERIES
FOR HIGH-FREQUENCY SEA LEVEL MONITORING**

crucial role in identifying and tracking surface water [2]. Additionally, satellites such as Landsat and Himawari-8 offer data in different resolutions, temporal intervals, and spectral ranges, as outlined in Table 1. For example, Landsat 8's OLI offers detailed spatial clarity at 30 meters but only updates every 16 days. Conversely, Himawari-8's AHI 8 provides frequent updates every 10 minutes but sacrifices spatial detail. Although these sensors are valuable, none can offer both high spatial and temporal resolutions simultaneously. To mitigate this constraint, blending imagery from multiple sensors has become increasingly popular.

TABLE 1. VARIOUS SATELLITES WITH CORRESPONDING RESOLUTIONS

| Name | Chanel/Band | Spectral (μm) | Spatial Resolution (m) | Termporal resolution |
|-------------|-----------------------|----------------------------|------------------------|----------------------|
| LANDSAT - 8 | Band 1 – 7 and band 9 | 0.433 – 2.290 | 30 m | 16 days |
| | Band 8 | 0.500 – 0.680 | 15 m | |
| | Band 10 and Band 11 | 1.060 – 1.251 | 100 m | |
| SPOT-5 | Green | 0.500 – 0.590 | 10 m | Daily |
| | Red | 0.610 – 0.680 | | |
| | NIR | 0.780 – 0.890 | | |
| | SWIR | 1.580 – 1.750 | 20 m | |
| | Panchromatic | 0.480 – 0.710 | 5 m | |
| Quickbird | B | 0.450 – 0.520 | 2.62 m | 1 – 3.5 days |
| | G | 0.520 – 0.600 | | |
| | R | 0.630 – 0.690 | | |
| | NIR | 0.760 – 0.900 | | |
| | Pan | 0.450 – 0.900 | 0.65 m | |
| Himawari-8 | B | 0.470 | 1000 m | 10 mins |
| | G | 0.510 | 1000 m | |
| | R | 0.644 | 500 m | |

Image fusion, a technique utilized in remote sensing, optimizes data collection by amalgamating images acquired from diverse sensors [3]. Image fusion algorithms are generally divided into two primary categories. The first category, referred to as spatial-spectral image fusion or pan-sharpening, integrates a low-resolution multispectral image with a high-resolution panchromatic image [4]. The second category, known as spatial-temporal image fusion, merges high spatial resolution data with high temporal resolution data to enhance both spatial and temporal resolutions [5]. This method leverages the strengths of sensors offering high temporal resolution alongside those providing medium to high spatial resolution.

Consequently, the main aim of this research is to investigate the viability of employing spatial and temporal image fusion techniques for effectively monitoring coastal dynamics and sea level changes. This objective will be achieved through three steps outlined in the subsequent section: firstly, generating 30-meter mNDWI images of the coastal region; secondly, evaluating the performance of the fusion results; and finally, assessing the water coverage. All details pertaining to these three steps will be discussed in the following section.

2. Research Method

This study investigates the practicality of blending satellite images for monitoring high-frequency fluctuations in sea levels. The workflow outlined in the methodology are shown in Figure 1.

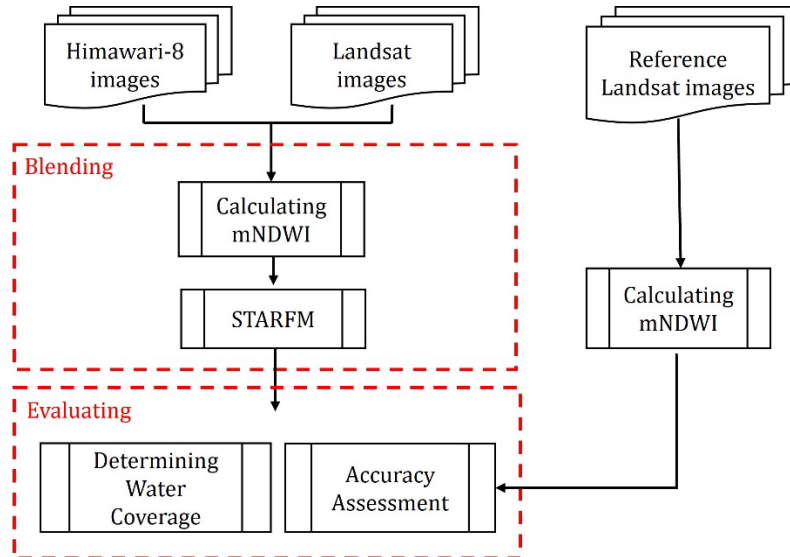


Figure 1. The methodology of the study

Figure 2 illustrates the various stages of this study, beginning with the initial phase of data collection, as detailed in Figure 2 below. Landsat 8 and Himawari-8 data are utilized in this research to achieve its objectives. After acquiring the data, the subsequent phase entails data processing, notably the application of Extract by Mask customized to the area of study as shown in Figure 4.

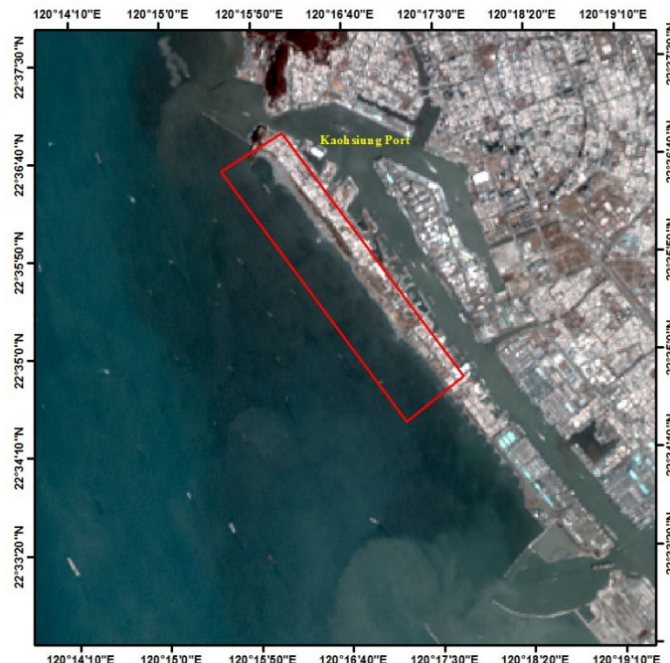


Figure 2. The Study Area of The Research

**THE FEASIBILITY OF FUSING SATELLITE IMAGERIES
FOR HIGH-FREQUENCY SEA LEVEL MONITORING**

The primary step of this research is divided into two segments: the blending section and the evaluation phase. In the blending section, vegetation density is calculated using a modified Normalized Difference Water Index (mNDWI). Once vegetation density is determined, mNDWI images from Landsat 8 and Himawari-8 are fused using the Temporal Adaptive Reflectance Fusion Model (STARFM). The final stage of this study involves the evaluation stage, which comprises two components: determining water coverage and conducting the accuracy assessments.

Channels or bands what we use is band Green (0.51 – 0.59 μm) and band 5 or SWIR (2.11 – 2.29 μm) for mNDWI calculations [6 - 9] as shown in Table 2. This research concentrates on the Kaohsiung Port of Taiwan. Following image acquisition, the Extract by Mask technique was used to isolate images of the study area from both Landsat and Himawari, as illustrated in Figure 3. This study seeks to assess the practicality of monitoring sea levels by employing the STARFM technique to integrate satellite imagery captured by various sensors, namely the Advanced Himawari Imager and Landsat 8. Specifically, the process of blending part involves calibrating and aligning all images within the study area, Kaohsiung Port, to surface reflectance through affine transformation.

After capturing images from both the Himawari and Landsat satellites, the next step involves utilizing specific bands of light known as the Green (G) and Shortwave Infrared (SWIR) bands as shown in formula (1). These bands are particularly useful for identifying water bodies due to their unique spectral characteristics. To quantify the presence of water, a metric called the Modified Normalized Difference Water Index (mNDWI) is calculated using the data from these bands. This index is a mathematical formula that compares the reflectance of light in the green and SWIR bands.

TABLE 2. CORRESPONDING BAND LIST OF LANDSAT OLI AND HIMAWARI-8

| Spectral Region | Landsat OLI Wavelength (μm) | Himawari -8 Wavelength (μm) | Landsat OLI Spatial Resolution (m) | Himawari-8 Spatial Resolution (km) |
|-----------------|-----------------------------|-----------------------------|------------------------------------|------------------------------------|
| Ultra Blue | 0.43 - 0.45 | - | 30 | - |
| Blue | 0.45 - 0.51 | 0.47 | 30 | 1 |
| *Green | 0.53 - 0.59 | 0.51 | 30 | 0.5 |
| Red | 0.64 - 0.67 | 0.64 | 30 | 1 |
| NIR | 0.85 - 0.88 | 0.86 | 30 | 2 |
| SWIR 1 | 1.57 - 1.65 | 1.61 | 30 | 2 |
| *SWIR 2 | 2.11 - 2.29 | 2.23 | 30 | 2 |

Once the mNDWI values are computed, a threshold value of 0.4 is applied to the results. This threshold serves as a boundary, allowing for the differentiation between areas that contain water and those that do not. When the mNDWI value exceeds 0.4, it indicates the presence of water, while values below 0.4 suggest non-water areas. This process is crucial for various applications such as monitoring changes in water bodies, assessing water quality, and managing water resources. Through the use of satellite imagery and sophisticated image processing methods, researchers and policymakers can obtain critical insights into the behavior of water bodies, enabling them to make well-informed decisions

about water management and conservation initiatives.

$$mNDWI = \frac{Green - SWIR}{Green + SWIR} \quad (1)$$

The second part of the blending section, the image fusion, applies the STARFM to predict the high temporal and spatial resolution. The STARFM algorithm is a sophisticated tool utilized in remote sensing, particularly for integrating satellite imagery obtained from different sources and time points. In its operation, STARFM requires specific datasets: images captured by both the Himawari and Landsat satellites, all acquired on a common reference time as detailed in Figure 3. Additionally, it utilizes the image of Himawari obtained at a predicted time along with the classification map from the reference time as the inputs. Importantly, all these datasets are represented in terms of water index values, which are numerical indicators revealing the presence or characteristics of water within the observed area.

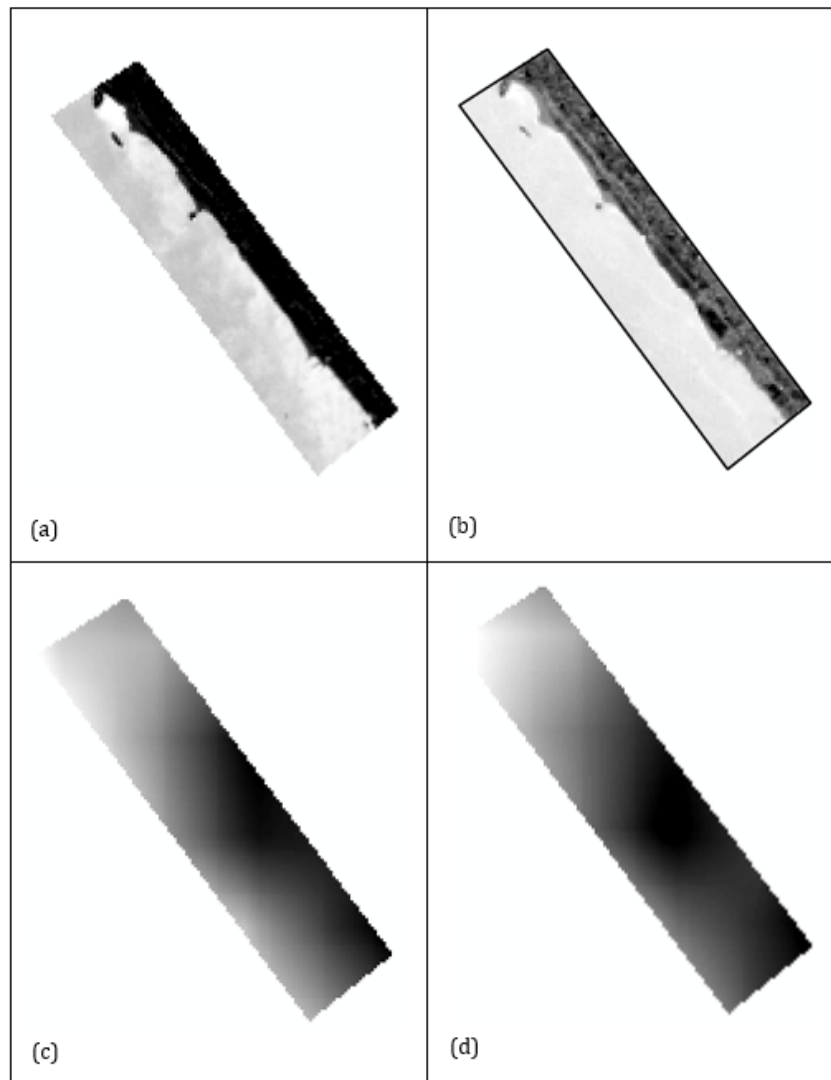


Figure 3. (a) mNDWI image of Landsat at the reference time. (b) mNDWI image of Himawari at the reference time. (c) mNDWI image of Landsat at the predicted time. (d) mNDWI image of Himawari at the predicted time

THE FEASIBILITY OF FUSING SATELLITE IMAGERIES FOR HIGH-FREQUENCY SEA LEVEL MONITORING

This methodological approach of STARFM aligns well with a previously established framework known as the Index-then-Blend approach. This methodology, as elucidated in prior research [10], follows a systematic sequence. Initially, it involves the computation of various indices, including water indices, which are tailored to highlight specific features or phenomena of interest, such as water bodies. Subsequently, the algorithm blends the information from the different datasets, integrating the water index values obtained from Himawari and Landsat imagery alongside the Landsat-derived classification map. By adhering to this sequential process, STARFM effectively harnesses the strengths of each dataset and ensures their harmonious integration, resulting in comprehensive and accurate outputs for further analysis and interpretation.

After the blending part, as the evaluation section of this study, the steps are divided to two evaluations, spatial evaluation and temporal evaluation. For spatial evaluation, some common accuracy assessments such as, Kappa Coefficient, Commission Error, Omission Error, and Overall Accuracy are calculated. On the other hand, the temporal trends are captured from the results of predicted time as the temporal evaluation. To obtain additional reference classification maps at varying water levels, it's necessary to acquire more than one Landsat image. Currently, our preliminary findings are based on just three nearly cloud-free Landsat images. Subsequently, for each Landsat date available, we initially utilize the existing Tide Model to determine water levels in the study area at 10:30 a.m.

Subsequently, all hourly Himawari-8 images from 09:00 a.m. to 03:00 p.m. on March 1, 2017, are gathered and the corresponding water height for each hour is determined. Table 3 presents the hourly water height data for March 1, 2017, which will serve as the reference image for the anticipated time. Depending on the chosen reference, we will subsequently obtain a 30-meter resolution image for each hour on this date.

TABLE 3. TIME POINTS OF HIMAWARI-8

| No | Reference Time |
|----|----------------|
| 1 | 09.00 a.m. |
| 2 | 10.00 a.m. |
| 3 | 11.00 a.m. |
| 4 | 12.00 p.m. |
| 5 | 13.00 p.m. |
| 6 | 14.00 p.m. |
| 7 | 15.00 p.m. |

Once all the aforementioned data is obtained, we proceed to match the water height of each hour from Himawari-8 with the water height of the Landsat image. If the water heights between the Landsat date and the corresponding time from Himawari-8 closely align, the Landsat image can be utilized to generate a classification map as the reference for predicting the high-resolution image at the matched hour as detailed in Table 4. To clarify, we can take the first instance at 09:00 a.m. For this, we utilized Himawari-8 and Landsat images at 10:30 a.m., along with the classification map, as reference images at the reference time. Then, the Himawari-8 image at the predicted time, 09:00 a.m., is utilized as the reference at the predicted time. This approach will be implemented for each corresponding pair mentioned below.

3. Results and Discussion

We examined the feasibility of blending the satellite imageries into two evaluations, spatial evaluation and temporal evaluation. Spatial evaluation focuses on assessing the

spatial accuracy and precision of the blended data. It involves examining how well the blended data aligns with actual spatial features and boundaries. Spatial evaluation may include measures such as Kappa Coefficient, Commission Error, Omission Error, and Overall Accuracy. The goal is to ensure that the blended data accurately represents the spatial characteristics of the area under study. Temporal evaluation, on the other hand, concerns the analysis of temporal consistency and stability over time. It involves investigating how well the blended data captures temporal trends of the predicted images. The objective is to verify the reliability and consistency of the blended data across different time periods.

1. Spatial Evaluation

To validate the results obtained from the Spatial and Temporal Adaptive Reflectance Fusion Model (STARFM), an actual Landsat image was utilized. This Landsat image served as a reference to compare and verify the accuracy of the predicted water map generated by STARFM. By overlaying the predicted water map with the water map derived from the Landsat image on a pixel-by-pixel basis, an evaluation map was created, as depicted in Figure 5 of the study. The evaluation map facilitated the identification of misclassified water areas, where discrepancies between the predicted and reference water maps were evident. These misclassifications often manifested as underestimations of water area, leading to a higher number of omission errors in the predicted water map. Several widely used accuracy assessment metrics, including commission and omission errors, overall accuracy, and the Kappa coefficient, were calculated from the evaluation map shown in Figure 4 and are summarized in Table 4 of the study.

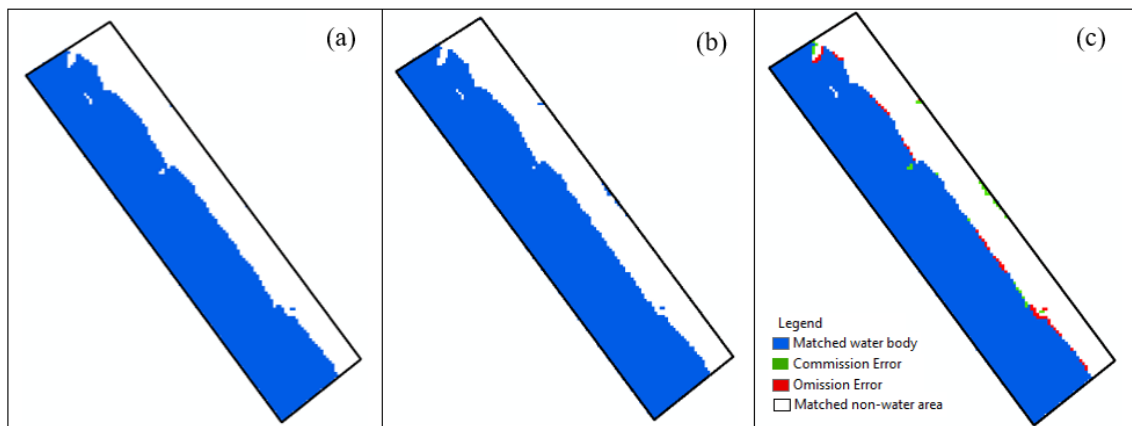


Figure 4. (a) The water map of the actual Landsat image at the reference time. (b) The water map of the result image at the predicted time (c) The evaluation map of the predicted

These indices provide quantitative measures to assess the accuracy and reliability of the predicted water map generated by STARFM. The values obtained for the accuracy evaluation indices as shown in Table 4, particularly the Kappa coefficient and overall accuracy, offer insights into the level of agreement between the predicted water map and the reference map derived from the actual Landsat image. High values of Kappa and overall accuracy indicate a strong consistency between the predicted and reference maps, suggesting that the predicted image generated by STARFM closely aligns with the actual water distribution captured by Landsat imagery.

**THE FEASIBILITY OF FUSING SATELLITE IMAGERIES
FOR HIGH-FREQUENCY SEA LEVEL MONITORING**

TABLE 4. THE ACCURACY OF SPATIAL EVALUATION

| Commission Error (%) | Omission Error (%) | Overall Accuracy (%) | Kappa Coefficient |
|----------------------|--------------------|----------------------|-------------------|
| 5.07 | 3.77 | 86 | 0.92 |

2. Temporal Evaluation

For temporal assessment, we juxtapose the water coverage with the water height recorded for each hour. Following the generation of predicted image results, pixel normalization is conducted using a threshold value of 0.4. Pixels with values equal to or greater than 0.4 are classified as water, while those below 0.4 are considered non-water pixels. This normalization divides the pixels into two categories, simplifying the calculation of water coverage and reducing processing time. Subsequently, water coverage is calculated based on the number of water pixels in each image and compared with water height data obtained from in-situ measurements (refer to Figure 5). This comparison operates on the assumption that higher water levels correspond to greater water coverage. The graph in Figure 6 illustrates the relationship between water coverage and water height. As water height increases, so does water coverage, while lower water heights correlate with reduced coverage. This evaluation suggests that STARFM aligns with this assumption.

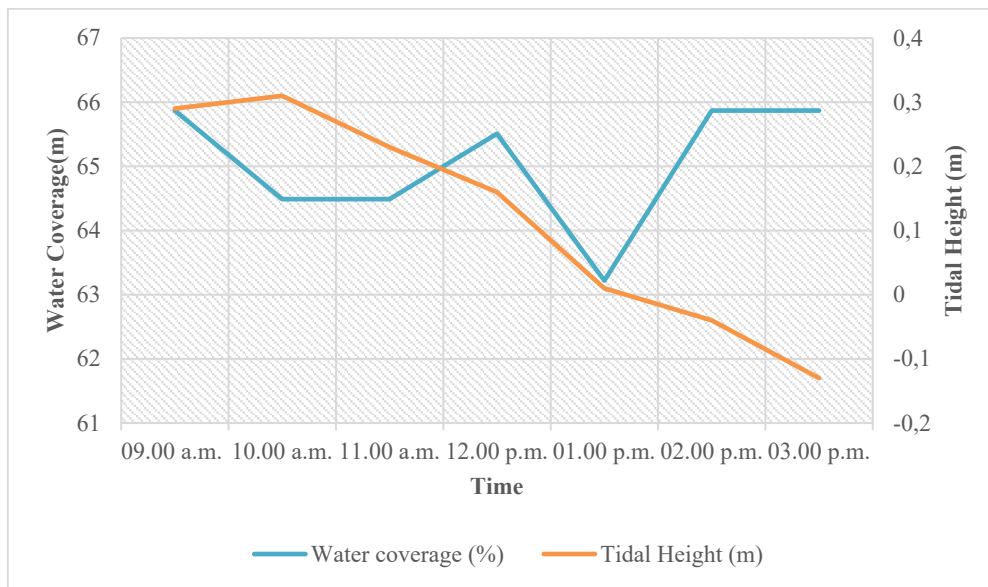


Figure 5. Temporal Evaluation result

4. Conclusion

This study suggests utilizing image fusion techniques to analyze and depict changes in sea levels along the coastline of Kaohsiung. Image fusion involves combining information from multiple images to create a single, enhanced image that provides more comprehensive insights into the landscape and environmental changes over time. By employing image fusion, the study aims to enhance the accuracy and detail of sea level change detection along the Kaohsiung coastline. The spatial evaluation of the study indicates that the Spatial and Temporal Adaptive Reflectance Fusion Model (STARFM) demonstrates effective performance in blending water index data. This suggests that STARFM successfully integrates information from different sources to produce blended images with accurate representations of water indices along the coastline. The temporal

evaluation reveals that the fused images do not accurately correspond to the observed water level data gathered in-situ. This discrepancy suggests a lack of alignment between the fused image data and the actual water level measurements over time. One possible explanation for this inconsistency is the utilization of a static classification map in the image fusion process. To address this issue, the study proposes a new direction for future research. Specifically, the historical data from Landsat satellites will be incorporated to develop a dynamic classification map that evolves over time. This approach aims to improve the accuracy of image fusion by accounting for changes in land cover and environmental conditions over different time periods.

References

- [1] B. S. Hague, R. B. Grayson, S. A. Talke, M. T. Black, & D. Jakob, *The effect of tidal range and mean sea-level changes on coastal flood hazards at Lakes Entrance, south-east Australia*. *Journal of Southern Hemisphere Earth Systems Science*, 73(2), 116-130. 2023.
- [2] C. Albertini, A. Gioia, V. Iacobellis, & S. Manfreda, *Detection of surface water and floods with multispectral satellites*. *Remote Sensing*, 14(23), 6005. 2022.
- [3] J. Xiao, A. K. Aggarwal, N. H. Duc, A. Arya, U. K. Rage, & R. Avtar, *A review of remote sensing image spatiotemporal fusion: Challenges, applications and recent trends*. *Remote Sensing Applications: Society and Environment*, 101005. 2023.
- [4] G. Yang, M. Zhou, K. Yan, A. Liu, X. Fu, & F. Wang, *Memory-augmented deep conditional unfolding network for pan-sharpening*. In *Proceedings of the IEEE/CVF conference on computer vision and pattern recognition* (pp. 1788-1797). 2022.
- [5] Y. Chen, K. Shi, Y. Ge, & Y. N. Zhou, *Spatiotemporal remote sensing image fusion using multiscale two-stream convolutional neural networks*. *IEEE Transactions on Geoscience and Remote Sensing*, 60, 1-12. 2022.
- [6] L. Chang, L. Cheng, C. Huang, S. Qin, C. Fu, & S. Li, *Extracting urban water bodies from Landsat imagery based on mNDWI and HSV transformation*. *Remote Sensing*, 14(22), 5785. 2022.
- [7] R. K. NH, *Study of fluctuations in surface area of Lake Haramaya using NDWI and MNDWI methods*. *JGISE: Journal of Geospatial Information Science and Engineering*, 5(1), 36-41. 2022.
- [8] J. Laonamsai, P. Julphunthong, T. Saprathet, B. Kimmany, T. Ganchanasuragit, P. Chomcheawchan, & N. Tomun, *Utilizing NDWI, MNDWI, SAVI, WRI, and AWEI for estimating erosion and deposition in Ping River in Thailand*. *Hydrology*, 10(3), 70. 2023.
- [9] O. S. Belhaj, S. T. Mubako, C. E. T. R. E. Aldouri, W. L. Hargrove, & E. A. Hadia, *Determination of change in surface waterbodies in the middle rio grande basin by modified normalized difference water index (MNDWI) 1994-2020, Libya*. *Jou. of Eco. & Enviro. Sci. and Tech*, 4(2), 67-80. 2022.
- [10] S. Park, N. W. Park, & S. I. Na, *An object-based weighting approach to spatiotemporal fusion of high spatial resolution satellite images for small-scale cropland monitoring*. *Agronomy*, 12(10), 2572. 2022.